

# VFTS682: a confirmed dynamical ejection?

M. Renzo<sup>1</sup> and ■ [TBD] ■.

Astronomical Institute Anton Pannekoek, University of Amsterdam, 1098 XH Amsterdam, The Netherlands

## ABSTRACT

**Key words.** stars: kinematics, stars: runaways, stars: individual: VFTS682

## 1. Introduction

■ [go to major star formation immediately] ■ ■ [sentence 2:debate of isolated or not] ■ ■ [paragraph 2 about ] ■ How do stars form is one longstanding question in astrophysics Lada & Lada (2003); Zinnecker & Yorke (2007). It is particularly difficult for massive stars, because these are intrinsically rare (e.g., Salpeter 1955; Kroupa 2001; Schneider et al. 2018), evolve fast, and remain enshrouded in their parent cloud during the formation process. Moreover, observations of young massive stars reveal a complicated multiplicity structure which requires explanation (Kobulnicky & Fryer 2007; Mason et al. 2009; Sana & Evans 2011; Sana et al. 2012; Kiminki & Kobulnicky 2012; Chini et al. 2012; Kobulnicky et al. 2014; Almeida et al. 2017; De Marco & Izzard 2017). Understanding massive star formation, possibly as a function of metallicity, is a key question given the present and upcoming transient survey (e.g., LSST, BlackGem, LIGO/Virgo O3 ) ■ [ref] ■ which will reveal transients associated to massive stars evolution and death.

The second data release (DR2) from the Gaia satellite (Gaia Collaboration et al. 2016, 2018) allows us to test these hypothesis using one particular star, VFTS682. This star is a very massive ( $M_{\text{ZAMS}} \simeq 150 M_{\odot}$ , Bestenlehner et al. 2011; Schneider et al. 2018) WNh5 star in the 30 Doradus region of the Large Magellanic Cloud (LMC), and it is presently observed at a projected distance of  $\sim 29$  pc from the nearest cluster of massive stars R136 (Bestenlehner et al. 2011). Based on the extremely high mass of this star and its present day apparent isolation, Bestenlehner et al. (2011) proposed it might be a candidate for isolated star formation, or a “slow runaway” ejected from R136 in the past. This second option is also supported by the N-body simulations of Fujii & Portegies Zwart (2011); Banerjee et al. (2012). Many other very massive stars are present in the surroundings of R136, and a more detailed analysis on the larger sample is desirable. ■ [this paper raised the debate/interest on VFTS682] ■

■ [vfts682 is interesting also because] ■

Massive stars can in principle be ejected from R136 as a consequence of dynamical interactions (Poveda et al. 1967; Leonard 1991; Evans et al. 2010; Fujii & Portegies Zwart 2011; Allison 2012; Oh & Kroupa 2016), or by the disruption of a binary by the first core-collapse supernova (Zwicky 1957; Blaauw 1961; De Donder et al. 1997; Eldridge et al. 2011; Renzo et al. 2018). However, R136 has an estimated age of  $\lesssim 2$  Myr (Sabbi et al.

2012), which is shorter than the shortest stellar lifetime ( $\sim 3$  Myr, e.g., Zapartas et al. 2017), so one would not expect the binary disruption scenario to be relevant for this cluster. ■ [move up] ■

In this study, we combine the radial velocity measurements from the VFTS survey (Evans et al. 2011) with the proper motion from Gaia DR2 to reconstruct the three-dimensional velocity of VFTS682, and test the hypothesis that this star was ejected from R136. We discuss in Sec. 2 the data for VFTS682, and the selection of stars used to define a local reference frame. Our results indicate that R136 is a bona fide runaway star (Sec. 3.1), therefore isolated star formation is *not* required to explain it. We also find that a dynamical ejection from R136 is compatible with the direction of its velocity vector. ■ [double check the following] ■ However, we find a mild discrepancy between the apparent age of VFTS682, its kinematic age, and the age estimates for R136 (Sec. 3.2). We conclude with a very brief discussion on the implications for theories of star formation, N-body interactions, and binary evolution in Sec. 4.

## 2. Gaia DR2 data selection

VFTS682 is labeled in the Gaia DR2 catalog<sup>1</sup> with the source id 4657685637907503744. The star has a `visibility_period` = 17, which counts how many observations have been used to reconstruct its astrometric solution (Lindgren et al. 2018). Its reported G-band magnitude is 15.65, cf. the V-band magnitude of 16.08 (Evans et al. 2011; Bestenlehner et al. 2011), and the reported `astrometric_excess_noise` = 0. These values suggest that the Gaia data for VFTS682 are trustworthy. However, the effective temperature reported in Gaia DR2 is one order of magnitude lower than what found by Bestenlehner et al. (2011), and the best fit parallax of this star is negative. We do not use the effective temperature of the star anywhere in this study, and we attribute the unphysical value of the parallax to the large distance to the LMC. Our main findings do not rely on the parallax nor the effective temperature values reported in the Gaia DR2 catalog.

We retrieve for VFTS682 the position in right ascension (RA) and declination (DE) in the ICRS frame (Gaia Collaboration et al. 2018), its proper motion components ( $\mu_{\text{RA}}$ , and  $\mu_{\text{DE}}$ , respectively). For the radial velocity of VFTS682 and of the 30

<sup>1</sup> <https://vizier.u-strasbg.fr/viz-bin/VizieR-3?-source=I/345/gaia2>

**Table 1.** Astrometric parameters for VFTS682. The peculiar radial velocity  $\delta v_{\text{rad}}$  is obtained as the difference between the average radial velocity of the 30 Doradus region ( $270 \pm 10 \text{ km s}^{-1}$ ) minus the radial velocity measured from the HeII  $\lambda 4686$  line for VFTS682 ( $315 \pm 15 \text{ km s}^{-1}$ ).

Parameter	Value	Source
RA [degree]	$84.73 \pm 0.03$	Gaia DR2
DE [degree]	$-69.07 \pm 0.05$	
$\mu_{\text{RA}}$ [mas yr $^{-1}$ ]	$1.84 \pm 0.07$	
$\mu_{\text{DE}}$ [mas yr $^{-1}$ ]	$0.78 \pm 0.08$	
$\delta v_{\text{rad}}$ [km s $^{-1}$ ]	$-45 \pm 25$	Bestenlehner et al. (2011)

Doradus region as a whole, we instead use the VFTS data as quoted in Bestenlehner et al. (2011). Table 1 lists the values adopted throughout this work for each of these quantities.

To compare the astrometry of VFTS682 and derive its peculiar motion, we then select data from the Gaia DR2 catalog for two regions: the “surroundings” of VFTS 682, and the “R136 cluster”. The surrounding region is defined by all the stars in a target of 10 arcminutes around VFTS682 fulfilling the following criteria: we require `visibility_period`  $\geq 5$ , `astrometric_excess_noise`  $< 1$ , the error on the proper motion components to be smaller than  $0.1 \text{ mas yr}^{-1}$ , and the proper motion components themselves to be smaller than  $2 \text{ mas yr}^{-1}$  in absolute value. At the distance to the LMC,  $1 \text{ mas yr}^{-1} \approx 250 \text{ km s}^{-1}$  (e.g., ?), so the cut on the values of the proper motions removes stars that would have projected tangential velocities in excess of  $\sim 500 \text{ km s}^{-1}$ , which are most likely to be foreground stars. We checked that the additional requirement of having parallaxes smaller than  $1 \text{ mas yr}^{-1}$  does not reduce further our sample. This selection yields 437 stars.

The “R136 cluster” is effectively defined by taking all the stars in a region of 50 arcseconds around R136a, one of the most massive members of the cluster itself (Crowther et al. 2010), requiring the same “quality” criteria applied above. This selection yields 42 stars. ■ **[improve definition of stars from R136, describe accordingly – check with Danny]** ■

Throughout this study, we assume the same distance of 50 kpc to the star, and to the 30 Doradus region as a whole.

For each of the two local rest frames (“surroundings” and “R136 cluster”), we compute the average transverse velocity as:

$$\langle \mu_i \rangle = \frac{\sum_{\text{stars}} \frac{1}{\Delta \mu_i} \mu_i}{\sum_{\text{stars}} \frac{1}{\Delta \mu_i}}, \quad \Delta \langle \mu_i \rangle = \frac{\sqrt{N}}{\sum_{\text{stars}} \frac{1}{\Delta \mu_i}}, \quad (1)$$

where  $i = \text{RA, DEC}$ , and  $\Delta \mu_i$  is the error on the proper motion component reported by Gaia, and the sums run over all the  $N$  stars of the frame considered. We evaluate each proper motion component separately.

The data retrieved, and the ipython notebook used for the analysis presented here will be made available at ■ **[probably git repo on bitbucket?]** ■.

### 3. The kinematics of VFTS682

#### 3.1. Is it a runaway star?

We first address the question of whether VFTS682 is a typical star from the kinematic point of view, or whether it is a runaway star with a significantly large peculiar velocity compared to its surrounding population. The former is what should be expected if it formed where we observe it today, in relative isolation from other massive stars.

Using the 437 stars selected as the “surrounding population” in Sec. 2 and shown in blue in Fig. 1, we find averaged proper motion components of  $\langle \mu_{\text{RA}}^{\text{sur}} \rangle = 1.695 \pm 0.003 \text{ mas yr}^{-1}$  and  $\langle \mu_{\text{DE}}^{\text{sur}} \rangle = 0.691 \pm 0.003 \text{ mas yr}^{-1}$ . Subtracting these values from the proper motions of VFTS682 (see Table 1), we obtain the components of proper motion of the star relative to the surrounding region  $\mu_{\text{RA}}^{\text{sur}} = 0.15 \pm 0.07 \text{ mas yr}^{-1}$  and  $\mu_{\text{DE}}^{\text{sur}} = 0.09 \pm 0.08 \text{ mas yr}^{-1}$ . These can be converted in the components of the transverse velocity  $v_{\text{RA}}^{\text{sur}} = 35 \pm 17 \text{ km s}^{-1}$ ,  $v_{\text{DE}}^{\text{sur}} = 22 \pm 19 \text{ km s}^{-1}$ , assuming a distance of 50 kpc (we do not account for the uncertainty in the distance estimate when propagating errors). The radial velocity from Bestenlehner et al. (2011) then gives the third component along the line of sight, allowing us to calculate the speed of the star:

$$v^{\text{sur}} = \sqrt{(v_{\text{RA}}^{\text{sur}})^2 + (v_{\text{DE}}^{\text{sur}})^2 + (\delta v_{\text{rad}})^2} = 61 \pm 22 \text{ km s}^{-1}. \quad (2)$$

This value for the three-dimensional speed of VFTS682 with respect to the surrounding stars make it a “bona fide” runaway star.

#### 3.2. Does it come from the R136 cluster?

The inset plot in Fig. 1 shows a zoom in of the region around R136 which includes VFTS682. Stars belonging to our “R136 cluster” group are shown in green (see Sec. 2), together with their proper motion as listed in the Gaia DR2 catalog. To test the hypothesis that VFTS682 was indeed ejected from this region, we check the orientation of its proper motion relative to these stars. We further consider also the kinematic age of the star.

We begin by evaluating the average proper motion for the stars representing the cluster. This is necessary to constrain the actual velocity obtained by VFTS682 at its ejection. By using Eq. 1 we find  $\langle \mu_{\text{RA}}^{\text{R136}} \rangle = 1.750 \pm 0.008 \text{ mas yr}^{-1}$  and  $\langle \mu_{\text{DE}}^{\text{R136}} \rangle = 0.742 \pm 0.009 \text{ mas yr}^{-1}$ . Therefore, using the values from Table 1, we obtain the components of the proper motion for VFTS682 relative to R136  $\mu_{\text{RA}}^{\text{R136}} = 0.09 \pm 0.07 \text{ mas yr}^{-1}$  and  $\mu_{\text{DE}}^{\text{R136}} = 0.04 \pm 0.08 \text{ mas yr}^{-1}$ . ■ **[improve numbers by selecting better sample]** ■. ■ **[discuss if direction is compatible. The error cone, obtained by propagating the errors on the proper motion components indicates that R136 is indeed the most likely origin, as expected by Fujii & Portegies Zwart (2011); Banerjee et al. (2012).]** ■

Assuming again a distance of 50 kpc and not considering the error on the distance, we can convert these into the components of the tangential velocity relative to R136,  $v_{\text{RA}}^{\text{R136}} = 21 \pm 18 \text{ km s}^{-1}$  and  $v_{\text{DE}}^{\text{R136}} = 10 \pm 21 \text{ km s}^{-1}$ . Finally, using the peculiar line of sight velocity from Bestenlehner et al. (2011), we obtain the three-dimensional peculiar velocity of VFTS682 with respect to R136

$$v^{\text{sur}} = \sqrt{(v_{\text{RA}}^{\text{R136}})^2 + (v_{\text{DE}}^{\text{R136}})^2 + (\delta v_{\text{rad}})^2} = 51 \pm 23 \text{ km s}^{-1}. \quad (3)$$

- **[number above not trustworthy]** ■
- **[kinematic age]** ■

### 4. Summary and Discussion

- VFTS682 is a bona fide runaway with  $v \sim 60 \text{ km s}^{-1}$  thrown out from R136. Both its speed and the age of the cluster are consistent with a dynamical ejection.

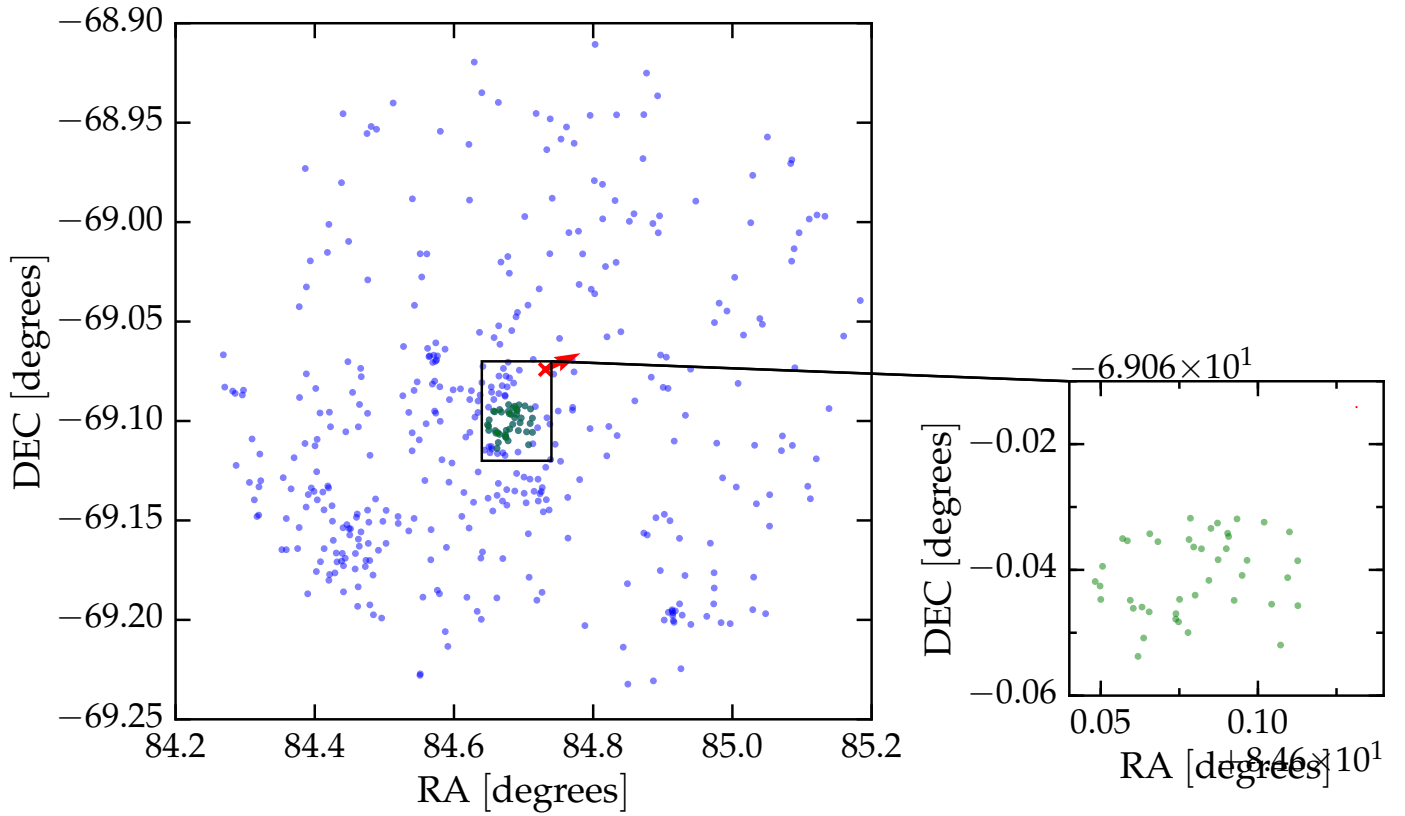


**Fig. 1.** The red cross indicates the position of VFTS682. Blue stars are those we use to define the generic “surroundings”, while the green dots indicate the stars we use to probe the core of R136, magnified in the inset. The red arrow shows the direction of the proper motion of VFTS682 relative to R136, and the gray shade indicates the uncertainty in the direction. ■ [orient properly, load picture on background, add cone of uncertainty, maybe show pm for all stars in inset?] ■

- VFTS682 comes from R136 as was expected by [Bestenlehner et al. \(2011\)](#); [Fujii & Portegies Zwart \(2011\)](#); [Banerjee et al. \(2012\)](#), so it does not require isolated SFH to be explained
- apparent age tension (connect to VFTS16 as well).
- is R136 a single young cluster or a merger
- estimate the influence of the gravitational potential of R136, what is its total mass and relaxation time?

Random notes:  $v \sin(i) < 200 \text{ km s}^{-1}$  from [Schneider et al. \(2018\)](#), age  $1.0 \pm 0.2 \text{ Myr}$  from [Schneider et al. \(2018\)](#)

## References

- Allison, R. J. 2012, MNRAS, 421, 3338
- Almeida, L. A., Sana, H., Taylor, W., et al. 2017, A&A, 598, A84
- Banerjee, S., Kroupa, P., & Oh, S. 2012, ApJ, 746, 15
- Bestenlehner, J. M., Vink, J. S., Gräfenr, G., et al. 2011, A&A, 530, L14
- Blaauw, A. 1961, Bull. Astron. Inst. Netherlands, 15, 265
- Chini, R., Hoffmeister, V. H., Nasser, A., Stahl, O., & Zinnecker, H. 2012, MNRAS, 424, 1925
- Crowther, P. A., Schnurr, O., Hirschi, R., et al. 2010, MNRAS, 408, 731
- De Donder, E., Vanbeveren, D., & van Bever, J. 1997, A&A, 318, 812
- De Marco, O. & Izzard, R. G. 2017, PASA, 34, e001
- Eldridge, J. J., Langer, N., & Tout, C. A. 2011, MNRAS, 414, 3501
- Evans, C. J., Taylor, W. D., Hénault-Brunet, V., et al. 2011, A&A, 530, A108
- Evans, C. J., Walborn, N. R., Crowther, P. A., et al. 2010, ApJ, 715, L74
- Fujii, M. S. & Portegies Zwart, S. 2011, Science, 334, 1380
- Gaia Collaboration, Brown, A. G. A., Vallenari, A., et al. 2018, ArXiv e-prints
- Gaia Collaboration, Prusti, T., de Bruijne, J. H. J., et al. 2016, A&A, 595, A1
- Kiminki, D. C. & Kobulnicky, H. A. 2012, ApJ, 751, 4
- Kobulnicky, H. A. & Fryer, C. L. 2007, ApJ, 670, 747
- Kobulnicky, H. A., Kiminki, D. C., Lundquist, M. J., et al. 2014, ApJS, 213, 34
- Kroupa, P. 2001, MNRAS, 322, 231
- Lada, C. J. & Lada, E. A. 2003, ARA&A, 41, 57
- Leonard, P. J. T. 1991, AJ, 101, 562
- Lindgren, L., Hernandez, J., Bombrun, A., et al. 2018, ArXiv e-prints
- Mason, B. D., Hartkopf, W. I., Gies, D. R., Henry, T. J., & Helsel, J. W. 2009, AJ, 137, 3358
- Oh, S. & Kroupa, P. 2016, A&A, 590, A107
- Poveda, A., Ruiz, J., & Allen, C. 1967, Boletín de los Observatorios Tonantzintla y Tacubaya, 4, 86
- Renzo, M., Zapartas, E., de Mink, S. E., et al. 2018, ArXiv:1804.09164
- Sabbi, E., Lennon, D. J., Gieles, M., et al. 2012, ApJ, 754, L37
- Salpeter, E. E. 1955, ApJ, 121, 161
- Sana, H., de Mink, S. E., de Koter, A., et al. 2012, Science, 337, 444
- Sana, H. & Evans, C. J. 2011, in IAU Symposium, Vol. 272, Active OB Stars: Structure, Evolution, Mass Loss, and Critical Limits, ed. C. Neiner, G. Wade, G. Meynet, & G. Peters, 474–485
- Schneider, F. R. N., Sana, H., Evans, C. J., et al. 2018, Science, 359, 69
- Zapartas, E., de Mink, S. E., Izzard, R. G., et al. 2017, A&A, 601, A29
- Zinnecker, H. & Yorke, H. W. 2007, ARA&A, 45, 481
- Zwicky, F. 1957, ZAp, 44, 64

**Acknowledgements.** The background image of Fig. 1 is based on observations made with ESO Telescopes at the La Silla Observatory under programme ID 076.C-0888, processed and released by the ESO VOS/ADP group. We are grateful to S. Torres for extremely useful discussions on the Gaia DR2 dataset.